Connections to Concrete-filled Tube Columns

Attaches à des colonnes formées de tubes remplis de béton

Anschlüsse an betongefüllte Hohlprofilstützen

P. ANSOURIAN

Senior Lecturer at the University of Sydney.

1. Introduction

The behaviour of circular concrete-filled tubes has been studied by P.K. NEOGI, H.K. SEN and J.C. CHAPMAN [1] who tested 18 tubes as pin-ended columns. They found that, for eccentrically loaded columns with L/d ratios greater than 15, good agreement existed between experiment and theory neglecting any triaxial effects caused by containment of the concrete by the steel. For shorter columns, triaxial effects raised the collapse load at small eccentricities, but the effect diminished with greater eccentricities. In the three columns with the smallest eccentricity $e/d = 0.05$, and $L/D \simeq 12$, the increase in collapse load was 23, 16 and 30 per cent respectively. In axially loaded column tests by P. GUIAUX and J. JANSS [2] in a testing machine with hemispherical bearings floating in oil under pressure, the six columns with L/d ratios less than 5.5 had collapse loads between 22 and 35 per cent over those computed from uniaxial properties only. The increase disappeared at L/d ratios greater than about 12.

Joints between hollow rectangular tubes have been investigated by R.G. REDWOOD [3] who tested welded joints between tubular beams and much wider tube columns. For this case, R.G. REDWOOD [4] also presented a finite difference analysis in an attempt to predict joint behaviour. More recently, B.L. MEHROTA and A.K. COVIL [8] analysed the problem of junctions between tubes of equal width. For these much more rigid joints, the authors' analysis provided values of joint modulus and of stress distribution in the elastic range. They also made the important observation that, because of shear lag in the beam "flanges", a major part of the load from the branch is carried to the column through the webs, whereas, with wide-flange sections, the load is transmitted largely through the flanges.

Simple connections between wide flange beams and square tube columns were investigated by R.N. WHITE and P.J. FANG [6]. These connections were of type recommended for A.I.S.C. Type 2 framing, for which no appreciable bending moment should be transmitted to the column. Five types of connection were tested,

two of which satisfied fully the requirements of shear strength, bending flexibility, and lack of damage to the tube wall. The others were either too stiff, or produced excessive local damage to the tube wall.

Tests of rigid welded connections between *I*-beams and concrete-filled circular tubes were reported by G. VALBERT [7]. In these tests, an axial load varying between half and the full squash load of the empty tube was applied to the column; the beam was then loaded until failure. Conclusions of a qualitative nature only were given, as there were uncertainties regarding the degree of fixity of the column supports. These were that the concrete was effective in delaying or preventing the appearance of buckles against the beam compression flange, and that failure occurred by tearing of the tube against the tension flange, in the neighbourhood of the welds.

The aims of the investigation presented here were firstly to study continuous frame connections between *I*-beams of normal and wide flange section and concrete-filled tubes, and secondly to study the detailed behaviour of rectangular tube columns under a range of axial loads and under the moment loading produced by a beam framing about one principal axis. In the eight tests with filled tubes, the ratios of maximum axial load to squash were chosen in the range 0.15 to 0.75. The ninth unit, tested with an empty tube, had a ratio of 0.53. Units 1 and 2 were manufactured with the welded and plated joints commonly used in connections to wide flange columns; units 3 and 4 were also welded, but the tension flange force was now applied as a compression to the back of the tube; units 5 to 9 contained shop-welded components, but the actual connection was effected by high strength friction bolting.

2. Description of Test Specimens

With the exception of specimen 9 which was empty, each specimen consisted of a 250 cm length of square tube filled with concrete and connected to a 100 cm length of *I*-beam of normal or wide flange section by one of the connections of Figs. 2 to 9.

Each tube was cut to length and its ends machined parallel. The dimensions were checked by measurement and by weighing. Offcuts were identified and used for the preparation of standard tensile tests pieces. Four threaded rods of 20 mm diameter and 400 mm length were supported at each end of the tube for eventual bolting to the supporting plates which transmitted the horizontal reaction during test (Fig. 1). For a yield of 1 cubic metre and a target strength of 0.35 T/cm^2 at 28 days, the concrete had the following composition:

River Gravel:	1300 kg
Rhine River Sand:	660 kg (0-2 mm)
Normal Portland Cement:	300 kg
Water:	180 litres

Cubes of 20 cm sides were cast for determination of crushing strength and prisms were used to measure the initial modulus. The ends of the tubes were kept closed for 28 days to prevent loss of water. No welding was done on the tube before the concrete was 15 days old.
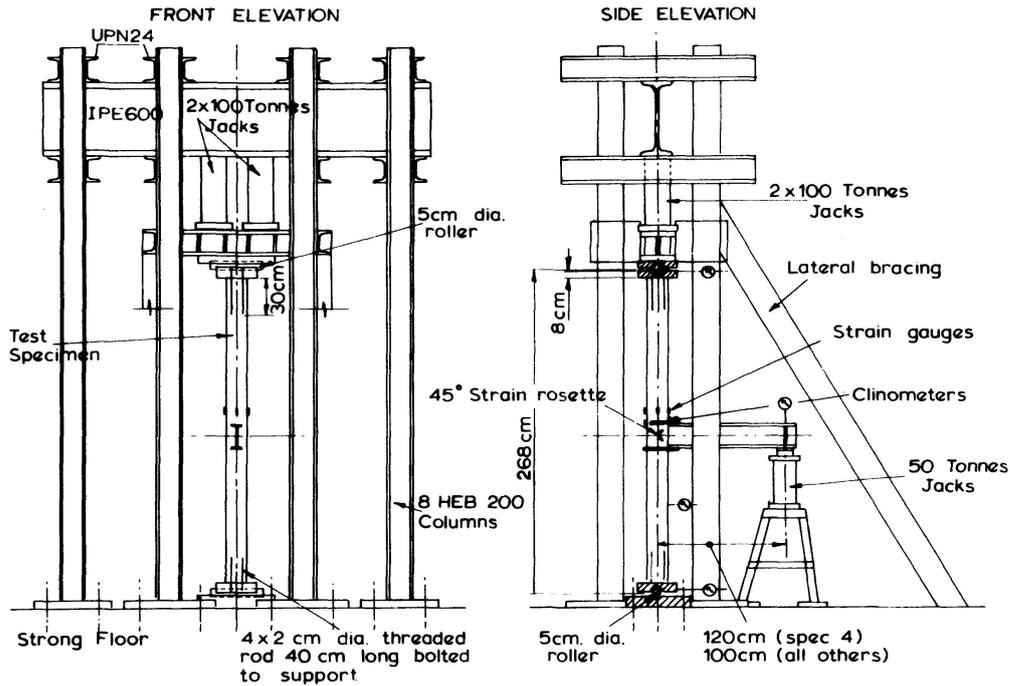
Fig. 1. Testing Layout.

Tube dimensions, beam identification and material properties of the steel and concrete are shown on Table 1. Details of each connection and dimensions of the European beam sections used are given on Figs. 2 to 9. The design of the connections was based on the development of the beam moment necessary to produce failure of the column for the axial load present, according to the theory presented in section 5. A brief description of each specimen follows.

Fig. 2.

Fig. 3.

In both specimens 1 and 2, the tension component of the beam couple was transmitted by a mild steel welded flange plate. In specimen 1, with a wide flange beam (HEB 180) of 18 cm width and depth, the plate was attached directly to the tube face by a full penetration V-butt weld. In specimen 2, with a beam (IPE 360) 36 cm deep and 17 cm wide, the butt weld was applied to a 1 cm thick backing plate welded on the tube face, i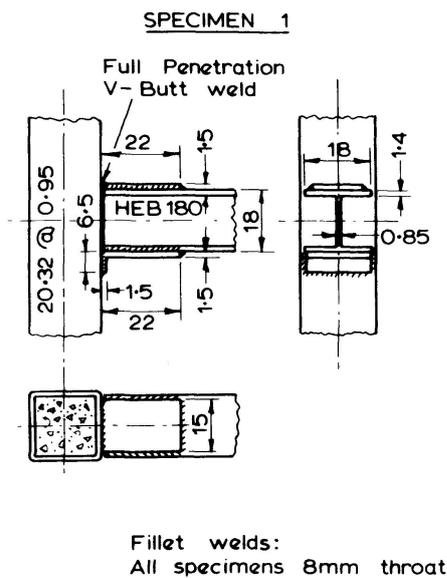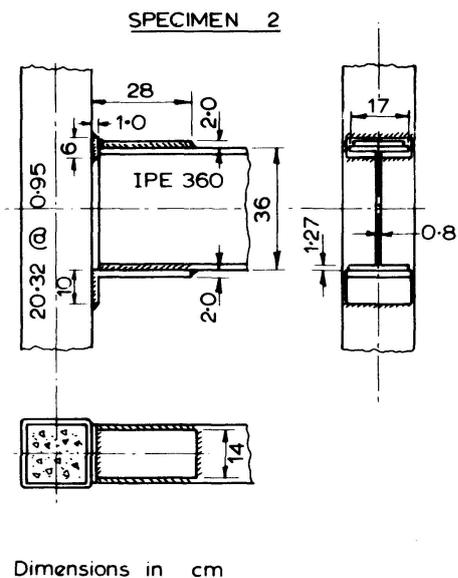n the hope of obtaining a weld capable of developing the yield force of the tension plate. The compression component of the beam couple, not critical in any of the tests was also transmitted by a welded plate. The beam shear force was carried by a shear plate.

After the evident failure of the V-butt weld to develop the yield force of the tension plate, all subsequent connections were designed to transmit that force as a compression on the back of the tube. This was done in specimens 3 and 4 by welding a U-shaped plate to the tension flange, and by welding two rectangular bars, as shown on Figs. 4 and 5, to complete the connection. A plate was welded to the column to help distribute the concentrated bar forces.
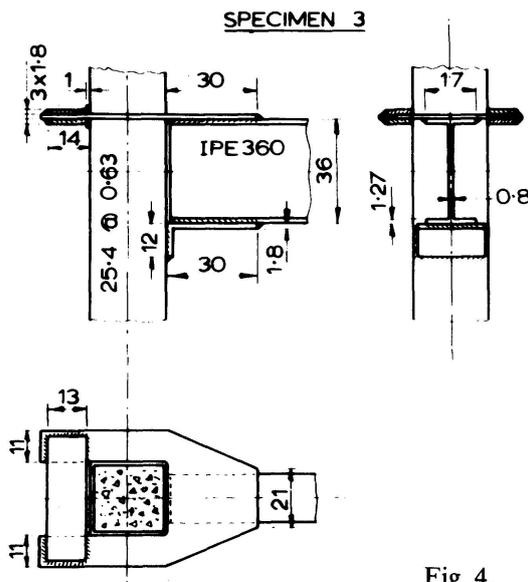
Fig. 4.
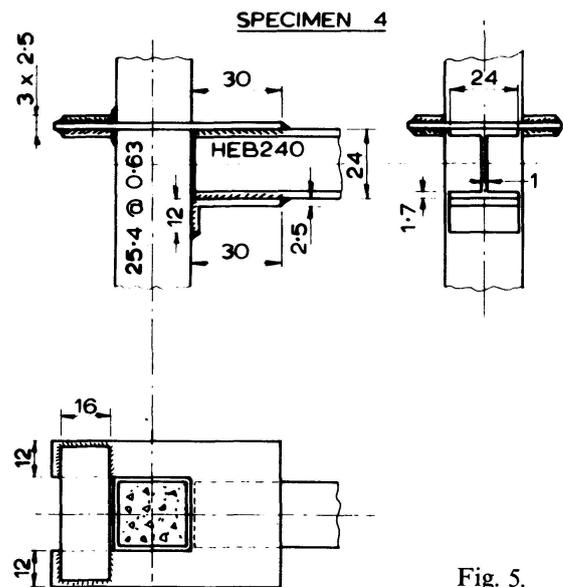
Fig. 5.

The connections of specimens 5-9 (Figs. 6-9) were designed so that all field operations would consist of high strength friction bolting. The bolts used were of 2 cm diameter, with an elastic limit of 9 T/cm², and were tensionned to a force of 15 T. The friction surfaces were prepared by cleaning with blowtorch and steel brush. The number of bolts used was based on the force to be transmitted at the theoretical failure load of the column. Specimen 9 was the only unit tested without concrete filling.

Fig. 6.

Fig. 7.

Fig. 8.

Fig. 9.
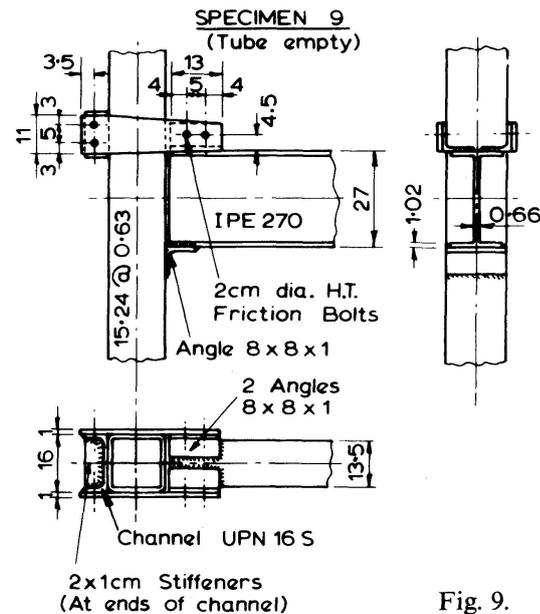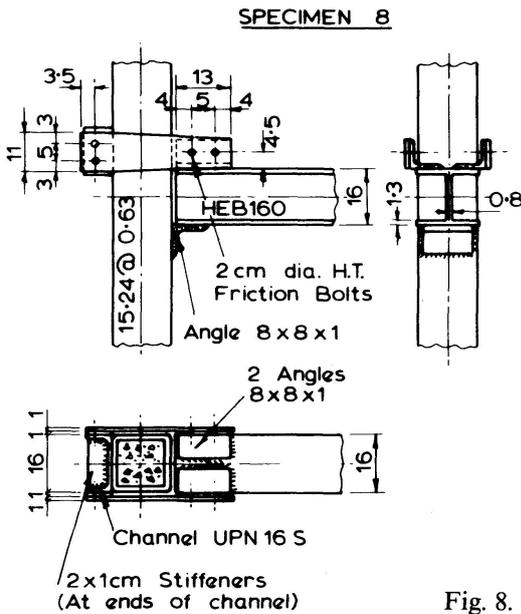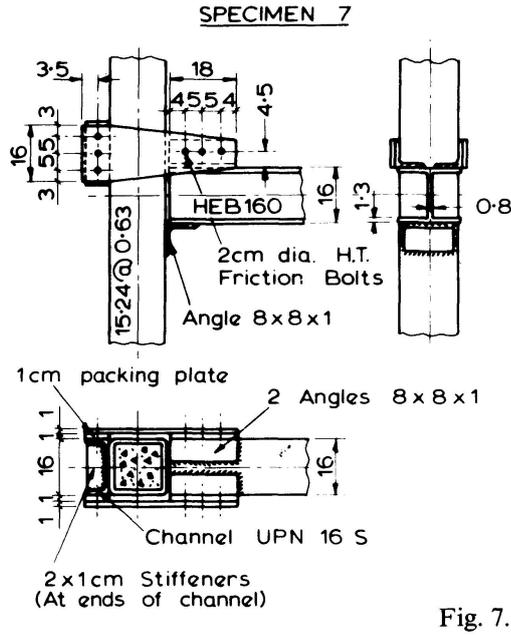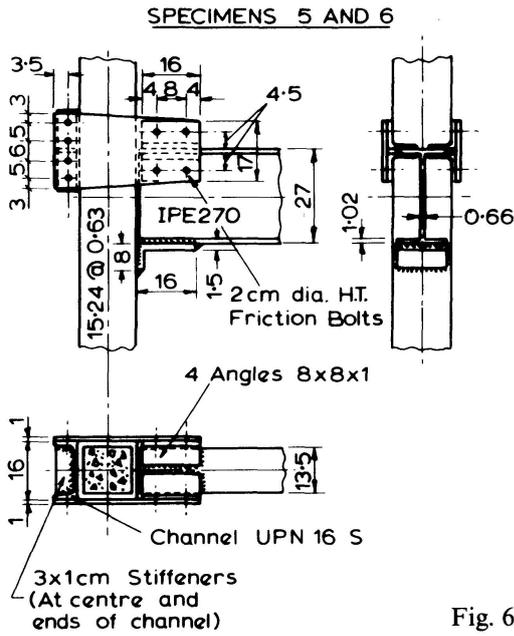
3. Experimental Procedure

After assembly, each specimen was centered in the testing apparatus shown on Fig. 1. One set of strain gauges was placed near the section of maximum moment, but sufficiently far from the beam shear plate to be unaffected by its local action. These gauges were intended to give a detailed distribution of column strains at or near the section of expected failure. A pair of 45-degree strain rosettes was placed at the centre of the tube webs to measure the effects of the connection shear. Other gauges were placed on specimens 1 and 2 near the V-butt welds in an effort to measure the local bending of the tube wall (Fig. 15).

A pair of clinometers was attached to the centreline of the tube at the level of the compression flange plate, to give measurements of rotation of the column at a section unaffected by distortions caused by the connection. The least count of the instruments was 1 second of arc, but the accuracy with which the bubble could be centered was approximately 5 seconds.

Dial gauges with a least count of $\frac{1}{100}$ mm. were used to measure deflections of the beam at the loading section, and to measure lateral movements of the bottom end plate of the column. Lateral movements of the top of the column, caused by the slight flexibility of the supporting structure, were measured on a scale attached to the column top plate, with a fixed theodolite.

The first step of the testing procedure was the application of the selected axial load to the column. A small trial load was applied and corresponding axial strains measured to verify that the load was uniformly distributed around the column. If significant departure from uniformity was detected, metal shims were inserted between the bottom roller and the base plate. The axial load was then applied in equal increments and held constant at the maximum value. For this purpose, two 100-tonne hydraulic jacks were used. Increments of beam load were then applied with a 50-tonne hydraulic jack until collapse occurred. The axial load in the lower half of the column was therefore reduced by the value of the beam load. For each increment, strains, clinometer and dial gauge readings were recorded. The duration of each test from the application of the axial load to collapse was approximately 2½ hours.

At the end of each series of tests, the corresponding concrete cubes were tested for crushing strength, and the prisms for initial elastic modulus. The steel coupons were tested in tension to give the average lower yield stress of each tube and beam. The values obtained are shown on Table 1.

4. Experimental Results and Comparison with Theory

Of the nine specimens tested, the first two failed by fracture of the V-butt weld connecting the tension flange plate to the tube. The third failed by buckling of the beam web after yielding of the connection plate. The remaining six failed by S-shaped collapse of the column after extensive yielding of the tube and varying amount of damage to the beam and connection. A description of the behaviour of each specimen is given hereunder; a summary of collapse loads is shown on table 2 and Fig. 10.

The clinometer readings were the most positive means of verifying the theory of column deformations given in section 5. The slope at the clinometers depended on the angle θ_A at the column top and on the deformations from the top hinge to the level of the clinometers, or, refering to Fig. 18,

$$\theta_{\text{CLIN.}} = -\theta_A + \int_o^{\frac{L-L_1}{2}} \rho \, dx = -\frac{1}{L} \int_o^L \rho \, (L-x) \, dx + \int_o^{\frac{L-L_1}{2}} \rho \, dx \tag{1}$$
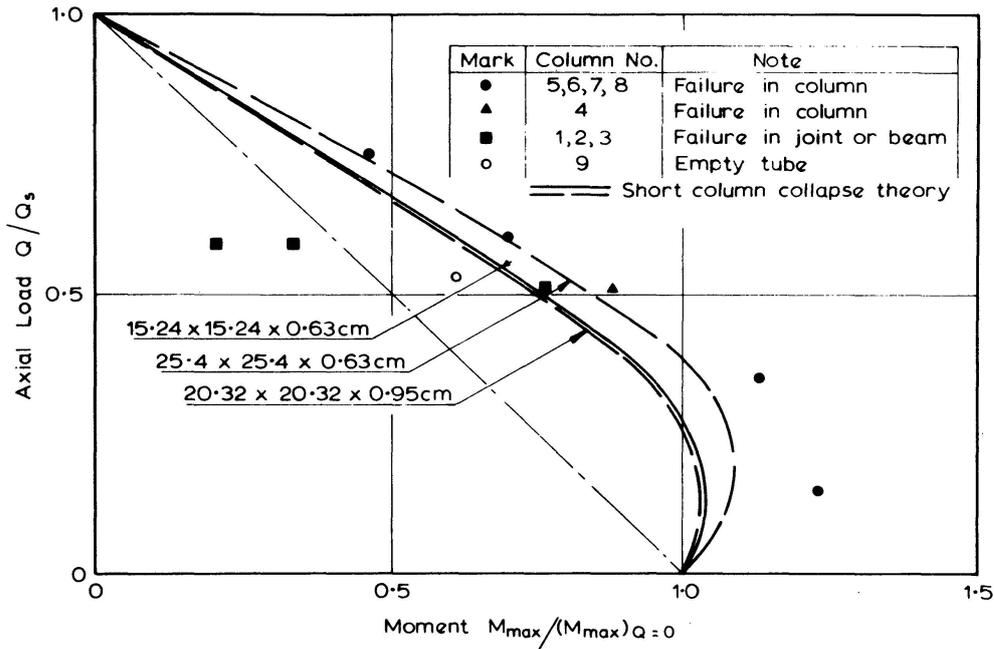
Fig. 10. Ultimate Load of Test Specimens.
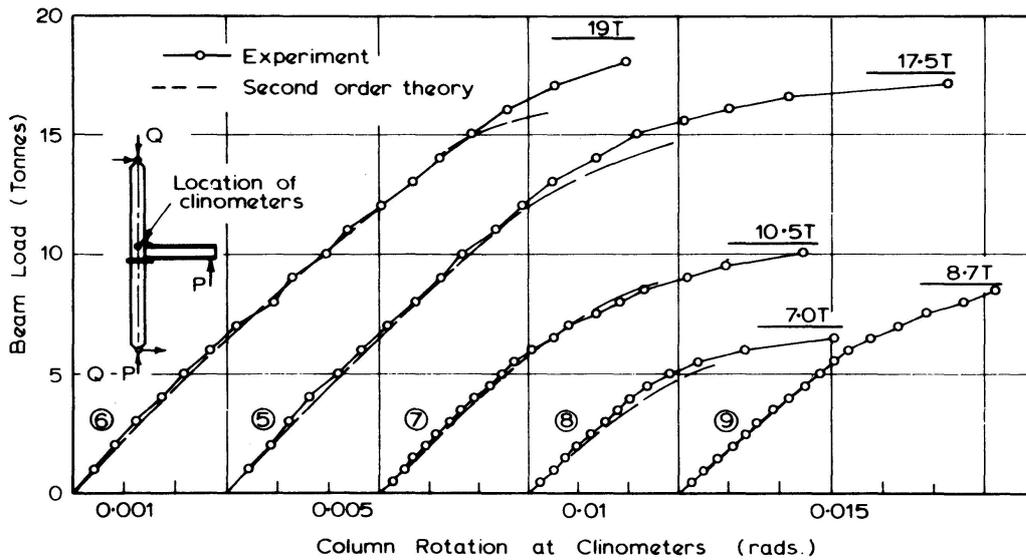
Fig. 11. Rotation of Specimens 5-9.

It may be seen on Fig. 11 that, up to high loads, there is generally very close agreement between the measured slopes and those computed from equ. (1). The predicted collapse load of the specimens that failed in the column were invariably conservative. An explanation of this may be that, near collapse, the concrete in the region of maximum bending and axial load did not behave according to the uniaxial properties assumed in the analysis, but was capable of supporting stresses higher than σ_m with the help of the confinement afforded by the tube. This effect may also have been enhanced by the gradient in bending moment distribution, as the moment decreased fairly rapidly away from the critical section. Strain hardening of the tube

steel was discarded as a possible explanation because the strain at the end of the yield plateau was measured to be greater than $10,000 \times 10^{-6}$ in the tensile coupon tests; average strains of this magnitude were detected neither on the column nor on the computer.
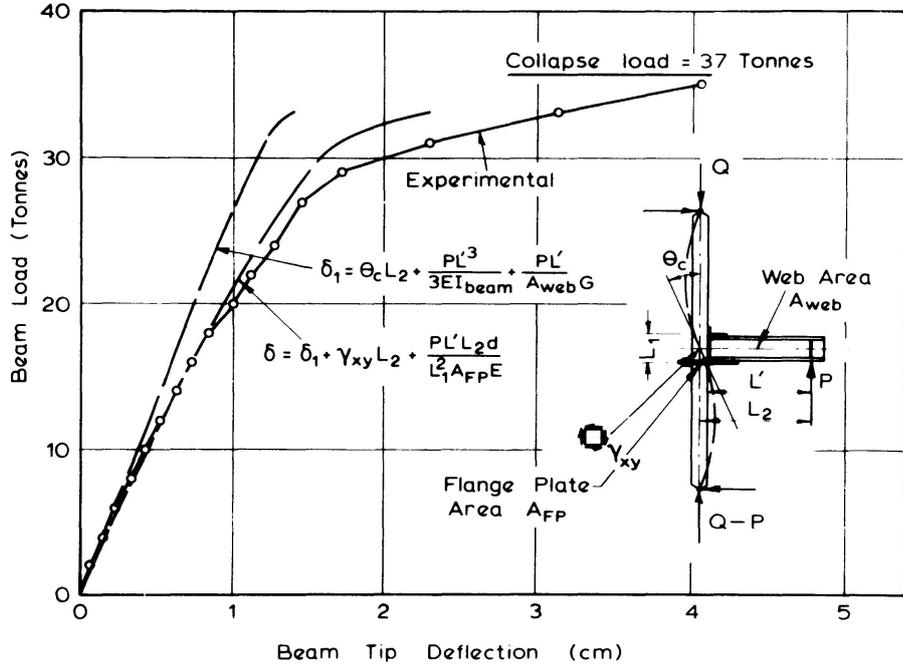
Fig. 12. Comparison of Deflection.

The axial strains measured near the section of maximum moment and axial load also compared well with those of the computer analysis. They are plotted together with results of the analysis on Fig. 13 (specimen 7). The large straining capacity of the filled tubular column was well demonstrated as strains of over $6,000 \times 10^{-6}$ were measured on the compression face of specimen 5.
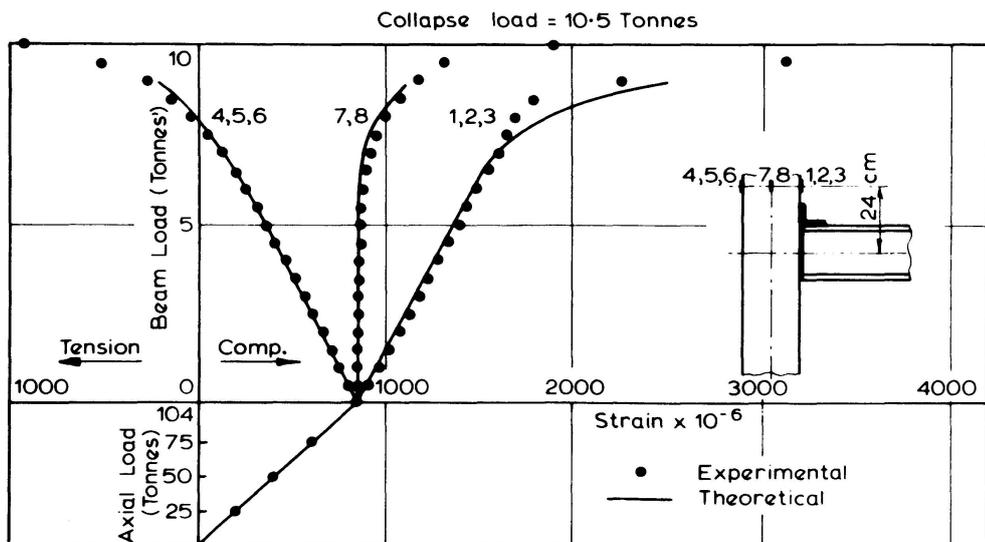
Fig. 13. Column Strains for Specimen 7.
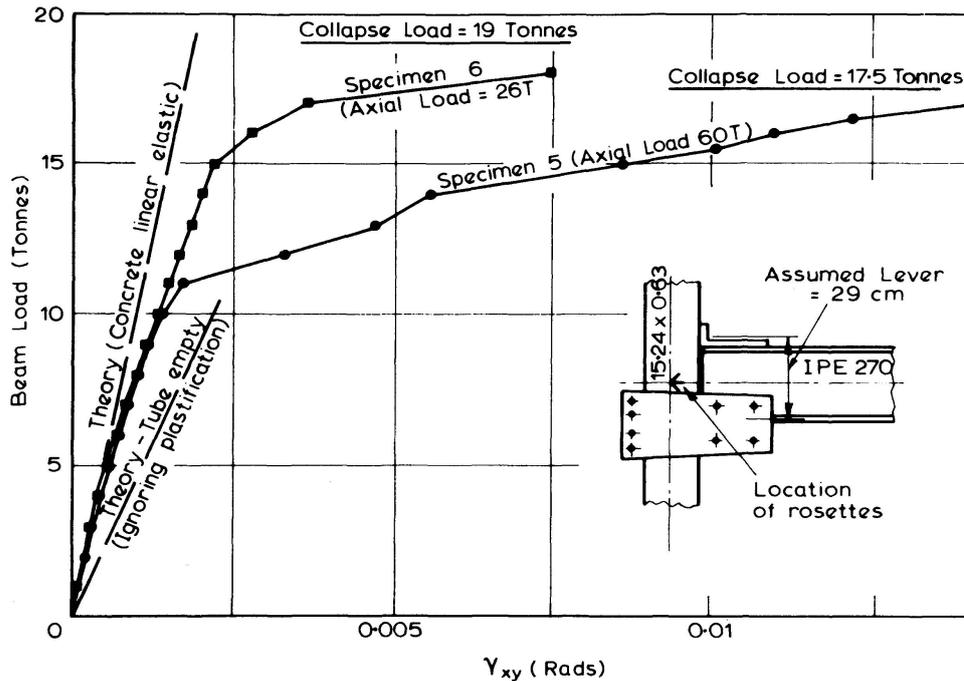
Fig. 14. Shear Strain at Connection.

The ninety degree strain rosettes were placed on each "web" of the column, at the intersection of the beam and column centrelines. They were a means of detecting the effects of the connection shear, and of assessing the contribution of the concrete filling in resisting it. Typical measured shear strains γ_{xy} in the horizontal direction, and comparison with simple theory are given on Fig. 14. Referring to Figs. 17 and 18, the connection shear is given by,

$$H = \frac{P}{LL_1}\left[L\left(L_2 - \frac{d}{2}\right) - L_1 L_2\right] \tag{2}$$

For an empty tube, the horizontal shear strain is,

$$\gamma_{xy} = \frac{H}{2ItG}\left[\frac{bt}{2}(d-t) + t\left(\frac{d}{2} - t\right)^2\right] \tag{3}$$

where $G = \dfrac{E}{2(1 + v)}$ = shear modulus of steel

and I = second moment of area of tube section.

The strains γ_{xy} measured in specimen 9 (empty tube) agreed with the strains calculated from equs. (2) and (3), with an error of less than 2 per cent up to 80 per cent of the collapse load.

Table 1: Description of Test Specimens.

SPECIMEN NUMBER	TYPE OF CONNECTION TO BEAM TENSION FLANGE	STEEL TUBE			STEEL BEAM		CONCRETE		COLUMN SQUASH LOAD $Q_s = A_s F_y + 0.83 A_c F_{cu}$	AXIAL LOAD Q	Q/Q_s
		DIMENSIONS	YIELD STRESS F_y	WIDTH THICKNESS	TYPE	YIELD STRESS	CUBE STRENGTH F_{cu}	MODULAR RATIO			
		cm	T/cm²		(See sketches For Dimensions)	T/cm²	T/cm²	-	Tonnes	Tonnes	
1	Plate welded to flange, and tube face with V-Butt weld.	20.32x20.32x0.95	3.14	21.4	HEB 180	3.0	0.38	7.7	339	200	0.59
2	Plate welded to flange, and to backing plate on tube face (full penetration V-Butt weld).	20.32x20.32x0.95	3.14	21.4	IPE 360	2.7	0.38	7.7	339	200	0.59
3	Plated welded U to back of tube column	25.4x25.4x0.63	3.36	40.3	IPE 360	2.7	0.38	7.7	396	200	0.51
4	Plated welded U to back of tube column	25.4x25.4x0.63	3.36	40.3	HEB 240	3.2	0.38	7.7	396	200	0.51
5	H.T. Friction bolting and welding	15.24x15.24x0.63	3.1	24.2	IPE 270	3.6	0.36	7.3	173	60	0.35
6	H.T. Friction bolting and welding	15.24x15.24x0.63	3.1	24.2	IPE 270	2.7	0.36	7.3	173	26	0.15
7	H.T. Friction bolting and welding	15.24x15.24x0.63	3.1	24.2	HEB 160	2.9	0.36	7.3	173	104	0.60
8	H.T. Friction bolting and welding	15.24x15.24x0.63	3.1	24.2	HEB 160	2.9	0.36	7.3	173	130	0.75
9	H.T. Friction bolting and welding	15.24x15.24x0.63	3.1	24.2	IPE 270	3.0	-	-	114	60	0.53

Table 2: Experimental and Theoretical Results.

| SPECIMEN NUMBER | AXIAL LOAD/SQUASH LOAD Q/Q_s | THEORY (SHORT COLUMN) | | | EXPERIMENT | | COLUMN FAILURE EXPERIMENT/THEORY | DESCRIPTION OF COLLAPSE |
		BEAM LOAD AT COLUMN COLLAPSE P_{max} Tonnes	BEAM LOAD AT COLUMN COLLAPSE For Q=0 $(P_{max})_{Q=0}$ Tonnes	$\frac{P_{max}}{(P_{max})_{Q=0}}$	BEAM LOAD AT COLUMN COLLAPSE P_{exp} Tonnes	$\frac{P_{exp}}{(P_{max})_{Q=0}}$	P_{exp}/P_{max}	
1	0.59	24.4	40	0.61	7.8	0.20	0.32	Rupture of V butt weld joining tension flange plate to tube face.
2	0.59	26.3	43	0.61	14	0.33	0.53	Rupture of V butt weld joining tension flange plate to backing plate on tube face.
3	0.51	44	53	0.83	40	0.76	0.91	Buckling of beam web after gross distortion caused by yielding of tension flange plate.
4	0.51	35	42	0.83	37	0.88	1.06	Failure of column in zone of high shear. Extensive yield of tube walls between beam flange plates.
5	0.35	14.7	15.5	0.95	17.5	1.13	1.19	General column failure initiated at zone of high moment and axial load. Slight yielding in beam.
6	0.15	16.0	15.5	1.03	19	1.23	1.19	General column failure initiated at zone of high moment and axial load. Extensive yielding of beam.
7	0.60	9.2	15.1	0.61	10.5	0.70	1.14	General column failure preceded by large beam deflections caused by deformation of connection channel.
8	0.75	5.9	15.1	0.39	7.0	0.46	1.19	General column failure.
9	0.53	8.7	14.3	0.61	8.7	0.61	1.0	General column failure followed by buckling and tearing of tube against compression flange.

In a concrete-filled tube, an estimate may be made of the initial resistance of the section to the shear H by assuming a fully composite and elastic section. If n is the modular ratio of the concrete, we have,

$$\gamma_{xy} = \frac{H}{I'b_{eff}G}\left[\frac{bt}{2}(d-t) + t\left(\frac{d}{2}-t\right)^2 + \frac{1}{2n}(b-2t)\left(\frac{d}{2}-t\right)^2\right] \tag{4}$$

where

$$I' = I + \frac{(b-2t)(d-2t)^3}{12\,n} \tag{5}$$

and

$$b_{eff} = \frac{b + 2t(n-1)}{n} \tag{6}$$

As the beam load is increased, the linear relationship ceases to hold, particularly at high axial loads. Allowance should then be made for the concrete non-linearity and fissuration, and for the eventual yielding of the tube walls under the combined axial and shear stresses. The most pronounced yielding in the connection shear zone was observed in specimen 4 which had the thinnest tube wall ($b/t = 40.3$) and the smallest lever arm ratio ($d/L_1 = 0.88$) of all the specimens that failed in the column. Even here, the appearance of the "shear" yield did not lead to immediate collapse of the column, but was the most likely cause of the smaller ratio of experimental to theoretical collapse shown on Table 2.

The assistance given by the concrete in resisting the shear force is illustrated on Fig. 14. At half the collapse load, the strain γ_{xy} was measured to be on average 57 per cent of the strain that would be measured on a corresponding empty tube, assuming the latter to remain elastic; in fact, without concrete filling, the columns would have yielded at low loads. As well as greatly increasing the axial and flexural resistance of the tube therefore, the concrete filling nearly doubled the shear stiffness of the tube.

After application of the axial load, the beam deflection measured at the load section was a function of all possible deformations of the tube, the beam and the connection. These deformations may be listed as:

(i)   rotation of the tube under flexure, in the presence of the axial load,
(ii)   shear deformation of the tube,
(iii) local deformations of the tube caused by the connecting plates,
(iv) elongation of the connecting plates,
(v)   slip at the bolts,
(vi) bending and shear deflection of the beam.

(i) and (vi) are sometimes regarded as the primary structural deformation while (ii) to (v) are lumped together to define the connector flexibility. Referring to the diagram in Fig. 15, the primary deformation is given by,

$$\delta_1 = \theta_c L_2 + PL'\left(\frac{L'^2}{3EI_{beam}} + \frac{1}{A_{web}G}\right) \tag{7}$$

where θ_c is computed from the theory of section 5.

If (iii) and (v) are neglected, the total deflection in the direction of the beam load becomes,

$$\delta = \delta_1 + \gamma_{xy} L_2 + \frac{PL'L_2 d}{L_1^2 A_{FP} E} \tag{8}$$

The last term of (8) was calculated for the elongation of the tension flange plate along the depth d of the column, assuming the centre of rotation to be in the base plate, at a distance L_1 from the tension plate.

A comparison between measured and computed deflections for specimen 4 is shown on Fig. 12. The agreement is generally good, indicating that most of the actual deformations are included in equ. (8). The remaining discrepancy at high loads is probably caused by local yielding of the tension flange plate, and by a slight penetration of the plates into the column.
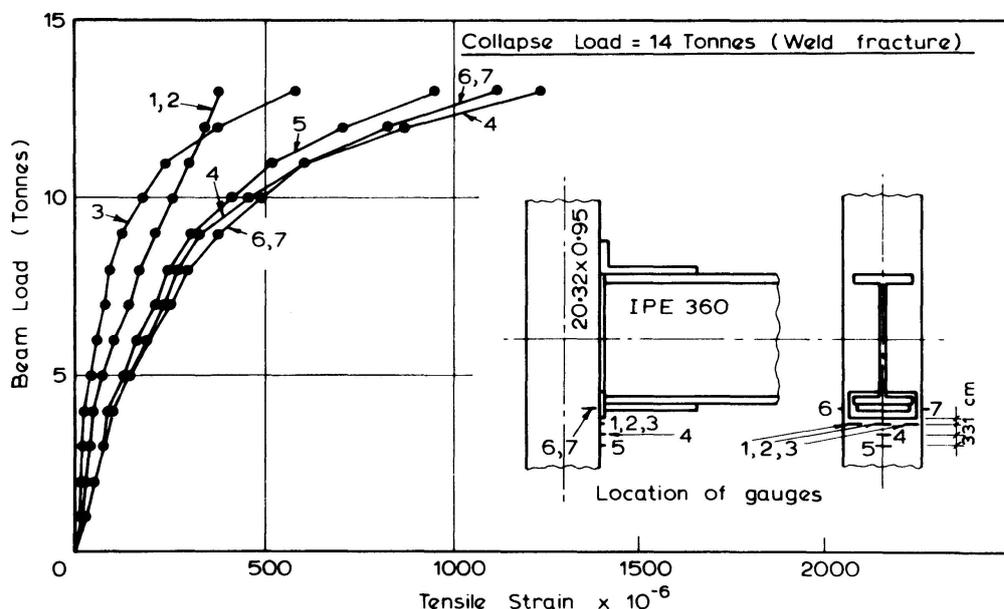
Fig. 15. Local Tube Strains Near Tension Plate (Specimen 2).

A detailed account of the behaviour of each specimen is given in the author's Ref. [10]. A summary is given in Table 2. The local distribution of strain on the front face of the tube near the tension connecting plate is shown on Fig. 15 (specimen 2). The distribution shows that the yield strain of the tube is reached on the side walls against the weld ends at relatively low beam loads.

5. Analysis of Concrete-Filled Rectangular Tube Columns under the axial load and Bending moment distribution existing in test program

A second-order, elasto-plastic analysis is presented for the behaviour of rectangular tube columns filled with concrete, and subjected to the axial load and bending moment distribution of the test program. The method has been programmed for

automatic computation to yield deformations up to collapse. The basic assumptions of the analysis are similar to those made by P.K. NEOGI, H.K. SENN and J.C. CHAPMAN [1]; these are:

(1) Plane sections before loading remain plane after loading; this implies complete interaction between steel and concrete.

(2) Each material is subjected to a uniaxial state of stress, neglecting all biaxial and triaxial effects which may arise.

(3) The stress-strain relation for the concrete in compression is represented by the equation

$$\frac{\sigma}{\sigma_m} = \frac{2\left(\varepsilon/\varepsilon_m\right)}{1 + \left(\varepsilon/\varepsilon_m\right)^2} \tag{9}$$

used by P. DESAYI and S. KRISHNAN [9], where σ_m is the maximum concrete stress in uniaxial compression and flexure, and is taken as 0.83 times the cube strength F_{cu}. ε_m is the strain corresponding to σ_m and is given by,

$$\varepsilon_m = \frac{2\sigma_m}{E_c} \tag{10}$$

where E_c, the initial slope, is obtained experimentally. Equ. (9) is plotted on Fig. 16(a).

(4) The tensile strength of the concrete is,

$$F_T = 0.059 \sqrt{\sigma_m} \tag{11}$$

where the units in this equation are in T/cm^2.

(5) The stress-strain relation for the steel is taken as bilinear, and is shown on Fig. 16(b).
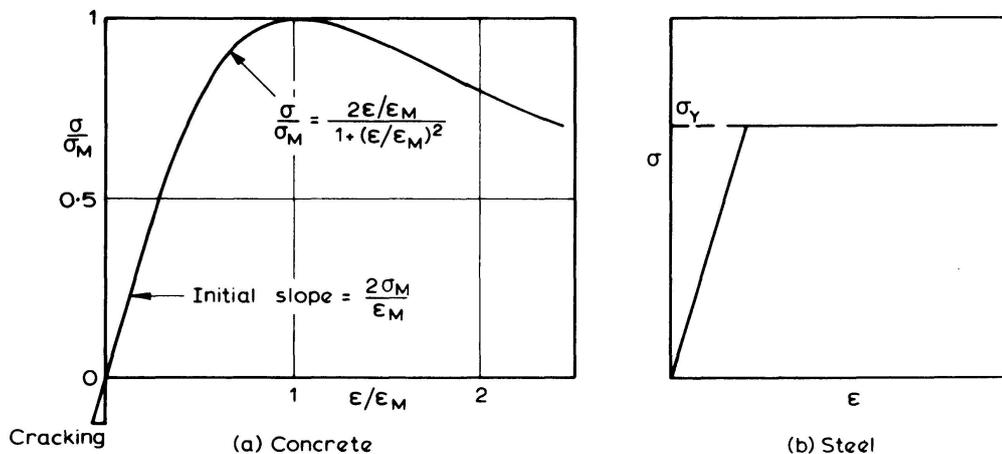

Fig. 16. Material Properties.

The expressions for neutral axis and moment of resistance for a given axial load Q and curvature ρ are obtained from a linear stress distribution by subtracting the effects of triangular, trapezoidal or analytical stress blocks corresponding to the non-linearity of the materials. The latter are the shaded areas of Fig. 17(c). The strain at mid-section is,

$$\varepsilon_c = \rho\left(k_2 d - \frac{d}{2}\right) \tag{12}$$

For axial equilibrium,

$$\varepsilon_c E\left(As + \frac{A_c}{n}\right) = Q \tag{13}$$

The neutral axis is located by,

$$k_2 d = \frac{d}{2} + \frac{Q}{\rho E\left(A_s + \frac{A_c}{n}\right)} \tag{14}$$
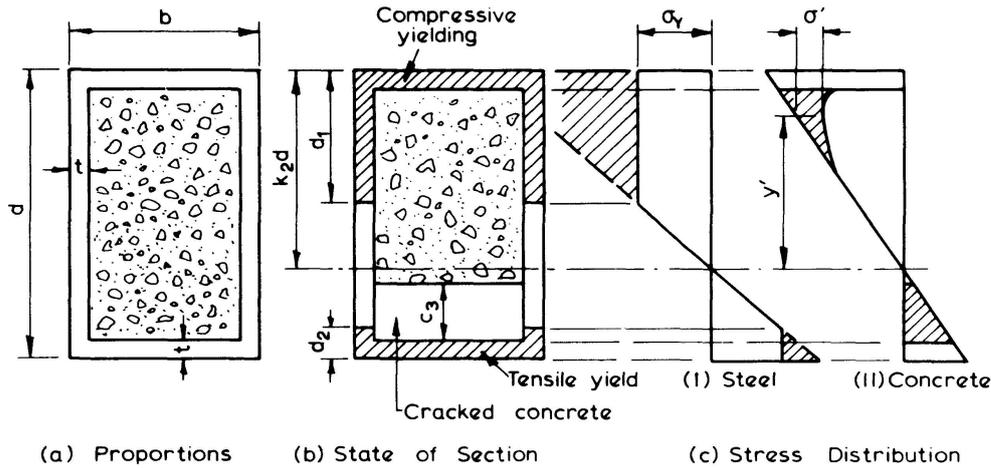
Fig. 17. Effect of Axial Load and Moment.

When compressive yielding extends into the web, the correction term is,

$$T_1 = \rho E\left[bt\left(d_1 - \frac{t}{2}\right) + (d_1 - t)^2\, t\right] \tag{15}$$

For tensile yielding into the web,

$$T_2 = \rho E\left[bt\left(d_2 - \frac{t}{2}\right) + (d_2 - t)^2\, t\right] \tag{16}$$

For cracking of the concrete on the tension side,

$$T_3 = \frac{\rho E}{n} c_3\, (b - 2t)\left(d - k_2 d - t - \frac{c_3}{2}\right) \tag{17}$$

and for the non-linearity of the concrete in compression,

$$T_4 = \int_0^{(k_2 d - t)} \sigma' (b - 2t) \, dy'$$

$$= (b - 2t) \left\{ \frac{\rho E}{2m} (k_2 d - t)^2 - \frac{\sigma_m \varepsilon_m}{\rho} \, \ln \left[1 + \frac{\rho^2}{\varepsilon_m^2} (k_2 d - t)^2 \right] \right\} \tag{18}$$

If $k_2 d > d - t$, the limits of integration are $(k_2 d - t)$ and $(k_2 d - d + t)$ and the expression becomes:

$$T_4 = (b - 2t) \left\{ \frac{\rho E}{n} (d - 2t) \left(k_2 d - \frac{d}{2} \right) - \frac{\sigma_m \varepsilon_m}{\rho} \, \ln \frac{1 + \frac{\rho^2}{\varepsilon_m^2} (k_2 d - t)^2}{1 + \frac{\rho^2}{\varepsilon_m^2} (k_2 d - d + t)^2} \right\} \tag{19}$$

The equation for axial equilibrium for the most general case may therefore be written as

$$\rho \left(k_2 d - \frac{d}{2} \right) \left(E A_s + \frac{E}{n} A_c \right) - T_1 + T_2 + T_3 - T_4 = Q \tag{20}$$

This is a complex implicit function of $k_2 d$ which may be solved iteratively for given Q and ρ.

A similar procedure is adopted to obtain expressions for moment of resistance M. In the uncracked linear case, we have,

$$M = \frac{\rho E}{12} \left\{ bd^3 - \frac{n - 1}{n} (b - 2t) (d - 2t)^3 \right\} \tag{21}$$

The correction terms are evaluated by taking moments of the forces corresponding to the shaded areas, about the central axis of the section. For yielding in the steel, they are,

$$S_1 = E\rho \left\{ \frac{bt}{2} \left(d_1 - \frac{t}{2} \right) (d - t) + \frac{bt^3}{12} + \frac{t}{2} (d_1 - t)^2 (d - t - d_1) + \frac{t}{6} (d_1 - t)^3 \right\} \tag{22}$$

for $t < d_1 < (d - t)$

$$S_2 = E\rho \left\{ \frac{bt}{2} (d_2 - \frac{t}{2}) (d - t) + \frac{bt^3}{12} + \frac{t}{2} (d_2 - t)^2 (d - t - d_2) + \frac{t}{6} (d_2 - t)^3 \right\} \tag{23}$$

for $t < d_2$

$$S_3 = \frac{E\rho}{n} \cdot c_3 (b - 2t) \left\{ \left(d - k_2 d - t - \frac{c_3}{2} \right) \left(\frac{d}{2} - t - \frac{c_3}{2} \right) + \frac{c_3^2}{12} \right\} \tag{24}$$

For non-linearity in the compression concrete, the correction term can again be calculated analytically. When the neutral axis is within the concrete, i.e. $k_2d < d - t$, we have,

$$S_4 = (b - 2t) \int_0^{(k_2d - t)} \sigma' \left\{ y' - \left(k_2d - \frac{d}{2}\right)\right\} dy' \tag{25}$$

After some manipulation, we find,

$$S_4 = -\left(k_2d - \frac{d}{2}\right)T_4 + (b - 2t)\left\{\frac{\rho E}{3n}(k_2d - t)^3\right.$$

$$\left.-\frac{2\sigma_m\varepsilon_m}{\rho}\left[k_2d - t - \frac{\varepsilon_m}{\rho}\text{ARCTAN}\left(\frac{\rho}{\varepsilon_m}(k_2d - t)\right)\right]\right\} \tag{26}$$

When the neutral axis is outside the concrete section, i.e. $k_2d > d - t$, we have,

$$S_4 = -\left(k_2d - \frac{d}{2}\right)T_4 + (b - 2t)\left\{\frac{\rho E}{3n}[(k_2d - t)^3 - (k_2d - d + t)^3]\right.$$

$$\left.-\frac{2\sigma_m\varepsilon_m}{\rho}\left[d - 2t - \frac{E_m}{\rho}\left(\text{ARCTAN}\left(\frac{\rho}{\varepsilon_m}(k_2d - t)\right) - \text{ARCTAN}\left(\frac{\rho}{\varepsilon_m}(k_2d - d + t)\right)\right)\right]\right\} \tag{27}$$

The final expression for moment of resistance therefore becomes,

$$M = \frac{\rho E}{12}\left\{bd^3 - \frac{n-1}{n}(b - 2t)(d - 2t)^3\right\} - S_1 - S_2 - S_3 - S_4 \tag{28}$$

The expressions for depth of yield in compression and in tension, and for the extent of cracking in the concrete are respectively given by:

$$d_1 = k_2d - \frac{\sigma_Y}{E\rho}$$

$$d_2 = d - k_2d - \frac{\sigma_Y}{E\rho} \tag{29}$$

$$c_3 = d - k_2d - t - \frac{.059n\sqrt{\sigma_m}}{E\rho}$$

At any stage of the second order column analysis, the curvature is required at each of the sections into which the column is divided, for a given applied moment and axial load. A variant of Newton's method was used to accelerate the convergence process. If the curvature ρ is required for moment M and axial load Q, the moment of resistance M, corresponding to a smaller curvature ρ_1 is calculated. The slope of the function is then estimated by calculating M_2 for a slightly greater curvature $\rho_2 = 1.05\,\rho_1$. A better estimate for ρ is then,

$$\rho_3 = \rho_1 + \frac{M - M_1}{M_2 - M_1} \times 0.05\,\rho_1 \tag{30}$$
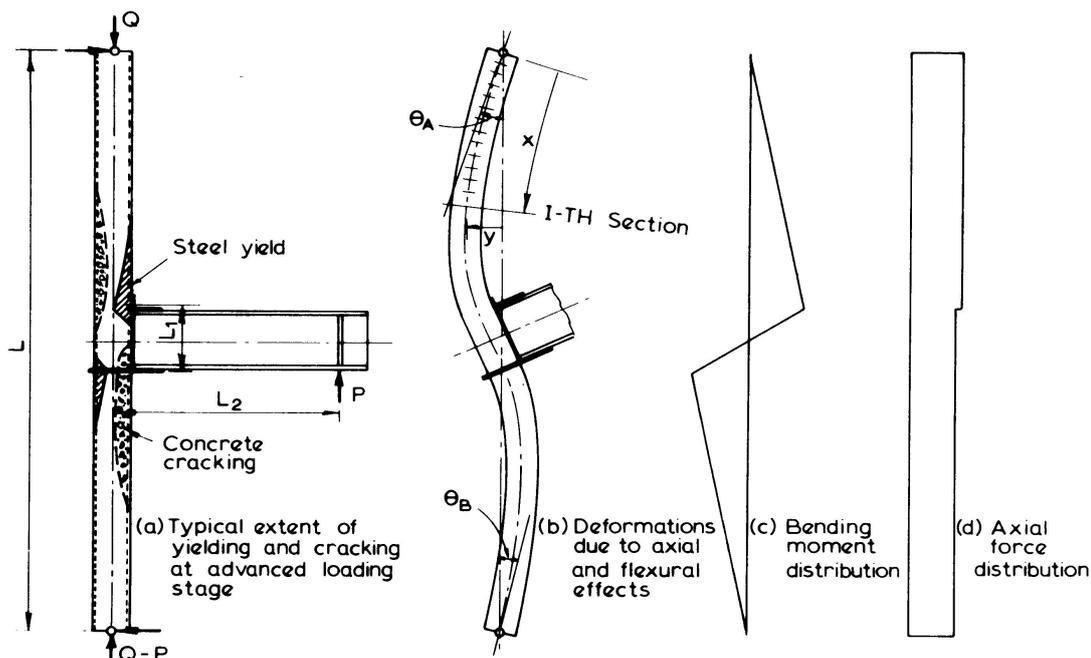
Fig. 18.

Referring to Fig. 18, the curvature is calculated at, say, fifty sections of the column. At section i, say in the lower portion of the column, the axial load and moment are,

$$Q' = -P$$

$$M_i = \frac{PL_2}{L}(x_i - L) + Q'y_i \tag{31}$$

The slope θ_A at the top of the column is given by:

$$\theta_A = \frac{1}{L} \int_0^L \rho(L - x)\, dx \tag{32}$$

or, by numerical quadrature,

$$\theta_A = \sum_{i=3,\,5,\,7\ldots}^{m-1} \frac{K}{3m} \left\{ L - \frac{6\, x_i\, \rho_{i-1} + (K - 6\rho_{i-1})\left(x_{i+1} - \frac{2}{3}\frac{L}{m}\right)}{K} \right\} \tag{33}$$

where $K = \rho_{i-1} + 4\,\rho_i{}^+ \rho_{i+1}$

The lateral deflection y at distance x from the top of the column is therefore,

$$y = \theta_A x - \int_0^x \rho\, (x - x')\, dx' \tag{34}$$

or numerically,

$$y_i = \theta_A\, x_i - \sum_{k=2,\,4,\,6\ldots}^{i} \frac{L}{3m} \left\{ 6\rho_{k-1}\, (x_i - x_k) + (K' - 6\rho_{k-1})\,(x_i - x_{k+1} + \frac{2L}{3m}) \right\} \tag{35}$$

where $K' = \rho_{k-1} + 4\rho_k + \rho_{k+1}$

An overall iterative loop is set up in the computer program, in which the deformed shape given by the distribution of y_i is recalculated until successive changes in y_i are sufficiently small.

As the number of iterations for convergence increases, the load increment ΔP is reduced, until convergence can no longer be attained; this defines the collapse load. Typical cycles of iteration are 3 at low loads and 8 near collapse.

6. Practical Considerations

In practice, filling the steel tubes with concrete has advantages which outweigh the additional cost of the filling. The principal gain is that of increased ultimate strength for the same column dimensions and weight of steel; the improvement is evident for all the structural actions acting on a column in a continuous frame: axial and shear force, and bending moment. At the same time, the stiffness of the column is significantly raised.

The ductility of an empty tube column is normally limited by local buckling of the wall under axial stress or under the action of the compression flange of a framing beam. In a conventional concrete column, the limit is set by crushing of the unconfined concrete. The mutual support of steel and concrete in a filled tube attached to the framing beam by an adequate connection results in an uncommonly ductile and tough structure which will remain integral under severe overload conditions, and may prove suitable under seismic or shock loading.

A disadvantage of the construction method is that the outside of the tube is exposed to the action of fire. While the concrete filling should improve the resistance of the bare tube by acting as a heat sink, it may be necessary to line the column with resistant sheeting where the fire risk is significant.

7. Conclusions

The behaviour of square tubular columns filled with concrete, framed on one side by an I-beam, and subjected to axial loads ranging from 0.15 to 0.75 times the squash load has been examined. Comparison of the experimental results obtained for the specimens that failed in the column, and of the computer analysis, led to the following conclusions:

(i) Full interaction between the steel and the concrete existed at all stages of loading.

(ii) Up to a compressive stress equal to σ_m, the concrete behaviour was in accordance with the Desayi and Krishnan curve, using measured values of the initial modulus, and taking the uniaxial compressive strength σ_m equal to 0.83 F_{cu}.

(iii) In the bending moment gradient existing in the tests, the contained concrete sustained stresses in excess of σ_m. This effect was evident at low or high superimposed axial loads.

(iv) The measured column collapse loads were from 6 to 19 per cent greater than the loads computed in the first order analysis. The lowest value of 6 per cent occurred in a column with thin walls ($b/t = 40.3$) and high connection shear. A summary is given on Fig. 10.

(v) The collapse loads were always greater than predicted from the second order analysis. The increase was a maximum of 30 per cent for the column with $Q/Q_s = 0.75$.

(vi) Failure of the columns was characterised by extensive yielding of the tube walls, and outward local buckling.

Two basic types of connection between the tubes and the normal or wide-flange beams were considered. These were welded connections to the front face of the tube, and connections in which the tensile component of the beam couple was applied as a compression to the back of the tube, to obtain maximum assistance from the concrete filling. Full welding and H.T. friction bolting were used in the second type of connection. The following conclusions were drawn from the study:

(i) Notwithstanding the relatively thick tubes used ($b/t = 21.4$), the V-butt weld connection to the front face of the tube, with or without backing plate, was not capable of developing the yield force of the tension flange plate. Because the tube face was much stiffer at the weld ends than at the centre, cracks were easily started and quickly led to rupture of the weld. This type of connection is therefore not recommended where high moment transmission is required.

(ii) Connections to the back of the tube, whether welded or bolted, were satisfactory. With distortion of the back channel prevented by adequate stiffening, most of the small flexibility of this type of connection could be explained in terms of the extension of the transmission plates and of the effects of the connection shear.

(iii) The shear strain γ_{xy}, caused by the connection shear force, could be predicted at low beam loads using the properties of the transformed section. Yielding under the action of this shear did not cause immediate collapse of the structure, but reduced the rigidity of the connection.

Finally, the important role of the concrete filling in helping the steel tube to resist the axial load, bending moment, shear force, and the local action of the connection, is again stressed.

8. Notation

A_c	Cross-sectional area of concrete.
A_s	Cross-sectional area of steel tube.
b	width of tube.
c_3	depth of cracking in concrete.
d	depth of tube.
d_1	depth of compression yielding in steel tube.
d_2	depth of tension yielding in steel tube.
E	Young's modulus of steel.
E_c	initial modulus of concrete.
F_{cu}	cube strength of concrete.
F_T	tensile strength of concrete.
G	shear modulus of steel.
H	connection shear force.
I	second moment of area.

$k_2 d$	neutral axis depth in tube column.
K	$\rho_{i-1} + 4\rho_i + \rho_{i+1}$.
K'	$\rho_{k-1} + 4\rho_k + \rho_{k+1}$.
L	length of column from pin to pin.
L'	distance from column face to beam load.
L_1	lever arm of beam moment.
L_2	eccentricity of beam load from column centreline.
M, M_i	bending moment.
m	number of subdivisions in column.
n	modular ratio of concrete.
P	beam load.
Q, Q'	axial load on column.
Q_s	squash load of column $= A_s \sigma_Y + 0.83 A_c F_{cu}$.
S_1, S_2, S_3, S_4	correction terms in moment of resistance calculation.
t	thickness of steel tube.
T_1, T_2, T_3, T_4	correction terms in neutral axis calculation.
x, x_i	distance along column from top hinge.
y, y_i	lateral deflection of column.
y'	distance above neutral axis of column.
δ	deflection.
ε	linear strain.
ε_c	strain at column centre.
ε_m	strain corresponding to peak stress in concrete.
γ	shear strain.
γ_{xy}	shear strain in coordinate directions.
σ	direct stress.
σ'	correction stress for concrete.
σ_m	maximum stress of concrete in uniaxial compression.
σ_Y	yield stress of steel.
θ_A	slope of column at top.
θ_B	slope of column at bottom.
θ_C	slope of column at centre.
ρ	curvature.
ν	Poisson's ratio.

10. Acknowledgements

9. References

1. Neogi, P.K., Sen, H.K., and Chapman, J.C.: Concrete-Filled Tubular Steel Columns — Uniaxial Behaviour Under Eccentric Loading. Construction Industry Research and Information Association, Technical Note 3, Jan. 1969.
2. Guiaux, P., and Janss, J.: Comportement au Flambement de Colonnes constituées de Tubes en Acier remplis de Béton. Rapport C.R.I.F., MT 65, Nov. 1970.
3. Redwood, R.G.: Behaviour of Joints between Rectangular Hollow Structural Members. Civ. Eng. and Pub. Wks. Review, Oct. 1965.
4. Redwood, R.G.: The Bending of Plate Loaded Through a Rigid Rectangular Inclusion. International Journal of Mechanical Sciences, Vol. 7, 1965.
5. White, R.N.: Framing Connections for Square and Rectangular Structural Tubing. A.I.S.C. Eng. Journ., Vol. 2, No. 3, July 1965.
6. White, R.N., and Fang, P.J.: Framing Connections for Square Structural Tubing. Proc. A.S.C.E., Journ. Struct. Div., Vol. 92, No. ST2, April 1966.
7. Valbert, G.: Essais d'Assemblages soudés d'une Solive sur un Poteau en Tube rempli de Béton. Construction métallique, 4 Dec. 1968.
8. Mehrotra, B.L., and Govil, A.K.: Shear Lag Analysis of Rectangular Full-Width Tube Junctions. Proc. A.S.C.E., Journ. Struct. Div., Vol. 98, No. STI, Jan. 1972.
9. Desayi, P., and Krishnan, S.: Equation for the Stress-Strain Curve of Concrete. Journ. A.C.I., Proc. 61, No. 3, March 1964.
10. Ansourian, P.: Rigid-Frame Connections to Concrete-Filled Tubular Steel Columns. C.R.I.F., Brussels, MT86, Jan. 1974.

Summary

Welded and bolted connections between I-beams and square tubes filled with concrete are examined in tests of nine structural units. The axial load on the columns has a range from 0.15 to 0.75 of the squash load. The deformations of the column are analysed in a second-order numerical analysis up to collapse.

Résumé

L'auteur présente neuf essais entrepris sur des attaches soudées ou boulonnées entre poutres en double T et tubes de section carrée remplis de béton. L'effort normal des colonnes se situe entre 15% et 75% de la charge d'écrasement. On étudie les déformations de la colonne jusqu'à la ruine à l'aide d'un calcul du second ordre.

Zusammenfassung

Geschweisste und geschraubte Anschlüsse von I-Trägern an betongefüllte quadratische Hohlprofile werden in Versuchen an neun Konstruktionseinheiten untersucht. Die Normalkraft der Stützen liegt zwischen 15% und 75% der Quetschlast. Die Stützenverformungen werden mittels einer Berechnung zweiter Ordnung ermittelt.